PERSPECTIVE
SOLID EARTH: GEODYNAMICS

Earth and Planetary Physics
9: 789–798, 2025
doi: 10.26464/epp2025056

Tomographic consistency in imaging lower-mantle plumes and their link to European Cenozoic Rift Volcanism

Chiara Civiero*, and Angelo De Min

Department of Mathematics, Informatics and Geosciences, University of Trieste, Trieste, Italy

Key Points:

- Several tomographic models reveal two broad low-velocity anomalies beneath Canaries (CEAA) and Central Europe (ECRA) connected near the base of the mantle.
- CEAA and ECRA are interpreted as two broad plumes rising from the top of the African LLSVP.
- The interaction of the ECRA material with the cold Alpine subducted slab hinders the vertical rise of the upwellings in the upper mantle.
- Deep-mantle plumes may play a role in the evolution of the European Cenozoic rift system and associated volcanism.

Citation: Civiero C and De Min A (2025). Tomographic consistency in imaging lower-mantle plumes and their link to European Cenozoic Rift Volcanism. *Earth Planet. Phys.*, *9*(4), 789–798. http://doi.org/10.26464/epp2025056

Abstract: A wide northeast-trending belt of intraplate alkaline volcanism, exhibiting similar geochemical characteristics, stretches from the Eastern Atlantic Ocean to the Cenozoic rift system in Europe. Its formation is associated with both passive and active mechanisms, but it remains a source of ongoing debate among geoscientists. Here, we show that seismic whole-mantle tomography models consistently identify two extensive low-velocity anomalies beneath the Canary Islands (CEAA) and Western-Central Europe (ECRA) at mid-mantle depths, merging near the core-mantle boundary. These low-velocity features are interpreted as two connected broad plumes originating from the top of the African LLSVP, likely feeding diapir-like upwellings in the upper mantle. The CEAA rises vertically, whereas the ECRA is tilted and dissipates at mantle transition zone depths, possibly due to the interaction with the cold Alpine subducted slab, which hinders its continuity at shallower depths. While plate-boundary forces are considered the primary drivers of rifting, the hypothesis that deep mantle plumes play a role in generating volcanic activity provides a compelling explanation for the European rift-related alkaline volcanism, supported by geological, geophysical, and geochemical evidence.

Keywords: European Cenozoic rift system; Canary Islands hotspot; rift-related volcanism; whole-mantle tomography; vote maps; large-scale plumes

1. Introduction

Continental rift systems are often linked to volcanism, with lithospheric extension during rifting considered a key factor in magma formation (Sengör and Burke, 1978). In the past, a net distinction was made between active and passive rifting. Active rifts are thought to be driven by a hot mantle upwelling while passive rifts develop in response to lithospheric thinning due to far-field stresses (McKenzie and Bickle, 1988; Wilson, 1992; Ziegler and Cloetingh, 2004). However, many continental rifts exhibit a combination of both mechanisms, thereby challenging this binary classification (Ruppel, 1995; Huismans et al., 2001; Merle, 2011; Koptev et al., 2021).

The European Cenozoic Rift System (or 'ECRIS') is one of the most extensively studied continental rifts, but the origin of its magmatism—whether from active mantle plumes, passive mantle ascent, or a combination of both mechanisms—remains controversial (Wilson and Downes, 1991; Wedepohl, 2000; Ziegler and Dèzes, 2005; Luijendijk et al., 2011; Mouthereau et al., 2021). The ECRIS extends from the North Sea coast to the Western Mediterranean and it finds its southern prolongation in south–east Iberia where younger, Quaternary products outcrop (Ziegler, 1992) (Figure 1). The graben structures of the rift include the Valencia Trough and the Olot Graben in the Iberian Peninsula, the Gulf of Lion, Saône, Limagne, and Bresse Grabens in southeastern France, the Rhine, Ruhr Valley, and Leine Grabens in Central Europe, and the Eger Graben in the Bohemian Massif. The rift evolved in the Alpine foreland from the late Eocene to recent times, coinciding with major Alpine orogenic phases (Figure 1). Around 30 Ma, slab roll-back-induced extension in the Western Mediterranean opened the Gulf of Lion and Valencia Trough, followed by the Liguro-Provençal, Alboran Sea, and Tyrrhenian basins (Comas et al., 1992; Lonergan and White, 1997; Jolivet et al., 1999).

Two distinct magmatic phases occurred in this geodynamic setting: (i) an orogenic-related phase with intrusive, subvolcanic, and volcanic rocks (from calc-alkaline to high K alkaline), and (ii)

Correspondence to: C. Civiero, chiara.civiero@units.it
Received 08 FEB 2025; Accepted 08 APR 2025.
First Published online 23 MAY 2025.

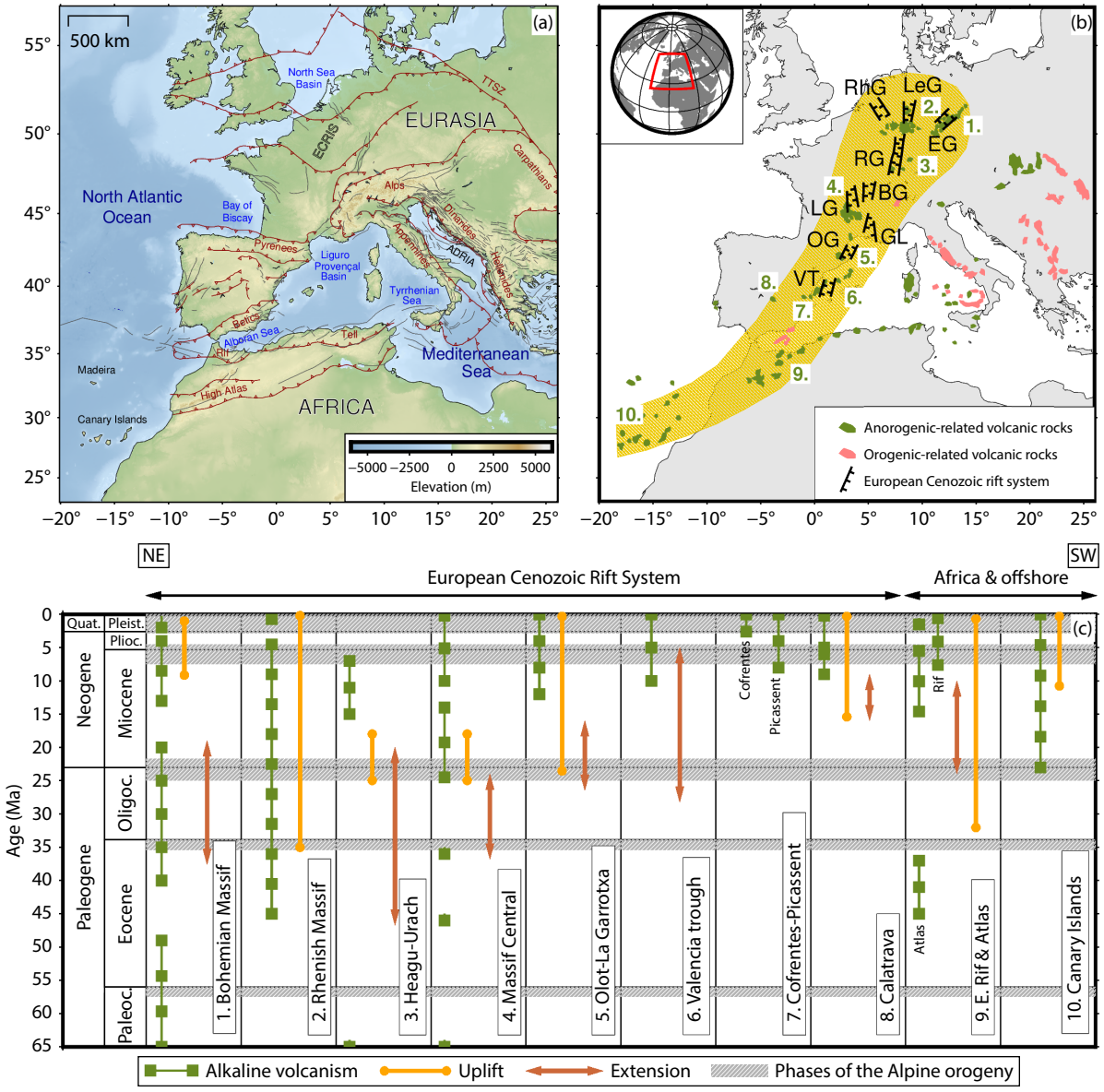

Figure 1. (a) Map of the study region showing the topography and major tectonic structures. Brown lines with ticks denote the main orogenic frontal zones, and the black, thin lines indicate the crustal faults. (b) Volcanism (green: anorogenic-related volcanic rocks; pink: orogenic-related rocks) and schematic rifting features: VT–Valencia Tough, OG–Olot Graben, GL–Graben of the Gulf of Lion, LG–Limagne Graben, BG–Bresse Graben, RG–Rhine Graben, RhG–Rhur Graben, LeG–Leine Graben, EG–Eger Graben. The yellow area indicates the spatial extent of the Cenozoic magmatism, including the ECRIS and the Moroccan Hot Line. Inset: the location of the study region is indicated with a red box. (c) Age of the igneous alkaline fields (numbered 1–10) plotted in panel B, along with localized uplift and extension from the Bohemian Massif in the northeast to the Canary Islands in the southwest.

an anorogenic phase, related to intraplate volcanics (mainly Na-alkaline) (Wilson and Downes, 1991; Harangi et al., 2006; Lustrino and Wilson, 2007) (Figure 1b). The latter phase encompasses both hotspot-driven and graben-associated volcanic pulses extending spatially from the Canary Islands and North Africa—along the so-called Moroccan Hot Line (Frizon de Lamotte et al., 2009)—towards the ECRIS area. Major European alkaline volcanic centers are located in uplifted areas across Iberia (e.g., at Calatrava, Cofrentes, Picassent, and Olot), the Valencia Trough, the Massif Central, the Rhenish Massif, the Rhine Graben, and the Bohemian Massif (see Figure 1), with peak activity during the Oligocene/Miocene and limited Quaternary activity. Very sparse volcanic manifestations occurred in the Paleocene at a pre-rift stage, likely resulting from lithospheric flexure due to early Alpine compression (Michon and Merle, 2001). Other volcanic areas, both anorogenic (e.g., Northern Italy and the Balaton region) and orogenic-related (e.g., Central-Southern Italy and the Pannonian Basin), also exist in the surrounding areas (Figure 1b). Although these rocks may have originated from the same source, they are not discussed in the text.

Overall, high surface heat-flow values are observed in the ECRIS and along the Hot Moroccan Line, with peaks of ~90 mW m^{-2} and above in Central and Western Europe (see zones 2–6 in Figure 2).

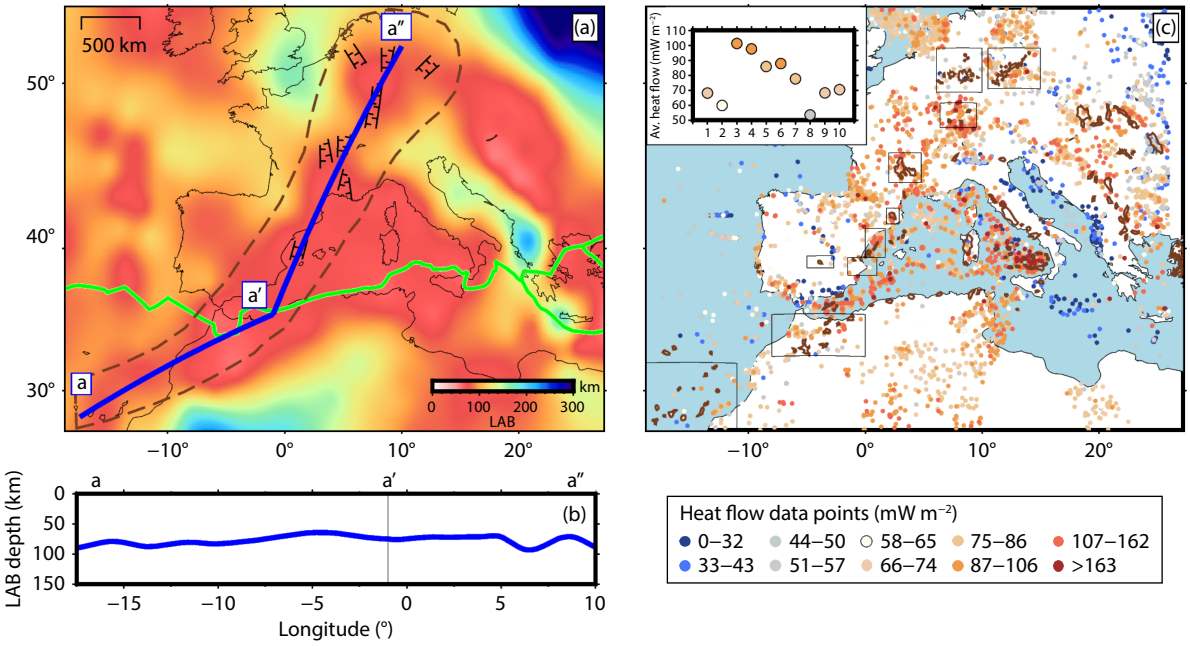

Figure 2. (a) Lithosphere–asthenosphere boundary (LAB) depth map based on the G-WINTERC model of Fullea et al. (2021). The lithosphere is relatively thin (~80 km depth) in the ECRIS and along the Hot Moroccan Line, whereas in adjacent regions, including the East European and West African Cratons, the LAB is deeper, reaching depths greater than 200 km. The dashed curve contours the region with Cenozoic magmatism. (b) Two profiles cutting the Hot Moroccan Line (a–a′) and the ECRIS (a′–a″). (c) Map of heat flow measurement points (Fuchs et al., 2021). Inset: the average heat flow values for the regions (black boxes) numbered 1–10 in Figure 1. Note that most of the regions of volcanism correspond to areas of high heat flux.

The correlation between heat-flow trends and the regions of weak, thin lithosphere (around 80 km thick) suggests that active mantle upwelling beneath Europe may contribute to the alkaline volcanism in areas with extended lithosphere (Goes et al., 2000a, b). This active scenario has been proposed as an additional mechanism, rather than an alternative to post-collisional passive processes, in weakening the lithosphere and controlling the level of rift-related volcanic activity (Ziegler and Cloetingh, 2004).

Tomographic models (e.g., Spakman et al., 1993; Granet et al., 1995; Ritter et al., 2001; Plomerová et al., 2007; Koulakov et al., 2009; Fichtner and Villaseñor, 2015; Zhu HJ et al., 2015) reveal localized sub-vertical upper-mantle low-velocity anomalies beneath the Massif Central, Rhenish Massif, Rhine Graben, and Bohemian Massif. Some authors (Granet et al., 1995; Goes et al., 1999; Ritter et al., 2001) interpret these features as small-scale plumes ("baby plumes"), possibly fed by a deeper mantle root.

Geochemical studies find that the isotope composition of the Cenozoic volcanic rocks of the Eastern Atlantic and Western-Central European domains is relatively uniform, and distinct from the mantle source for MORB supporting the hypothesis of a single lower-mantle origin from a well-mixed reservoir (Hoernle et al., 1995; Haase et al., 2004; Buikin et al., 2005). In contrast, the petrogenetic analysis of Lustrino and Wilson (2007) suggests that all anorogenic magmatic events originate from an asthenospheric source displaying HIMU isotopic signatures and local lithospheric contamination, without requiring a deep mantle root. Given the complexity of the Eurasian–African plate collision and the challenges in imaging the lower mantle, the idea that a deep mantle plume triggers asthenosphere-derived partial melting remains highly debated.

This study explores deep mantle structure beneath Europe by analyzing a global-scale full-waveform inversion tomography model recently published by Thrastarson et al. (2024). Additionally, we apply a 'voting' process to identify common large-scale features—such as size, shape, and position—across various seismic tomography models. The consistent observation of two low-velocity mantle anomalies beneath the Eastern Atlantic and Central Europe, converging near the core-mantle boundary, suggests that the ECRIS and Canary Islands may share a common source of plume-like volcanism.

2. Mantle Plumes Imaged by Seismic Tomographic Models

Seismic tomography is a powerful geophysical tool used to image the Earth's interior by analyzing the travel times and amplitudes of seismic waves. However, tomographic models differ in the seismological measurements, methods, and inversion schemes that vary in wave propagation approximations, model parameterization, and regularization choices, and the range of seismic phases used (e.g., Masters et al., 1982; van der Hilst et al., 1997; Rawlinson and Sambridge, 2004; Boschi et al., 2007; Liu Q and Gu YJ, 2012).

The newly developed "REVEAL" model by Thrastarson et al. (2024) offers an up-to-date approach to imaging the Earth's mantle using a transversely isotropic full-waveform inversion and incorporating both surface and body wave data. Figure 3 presents depth slices from this model of the mantle (600–2700 km depth) beneath Europe, providing fresh insights into the deep velocity structures. The slices show a broad low-velocity anomaly centered beneath

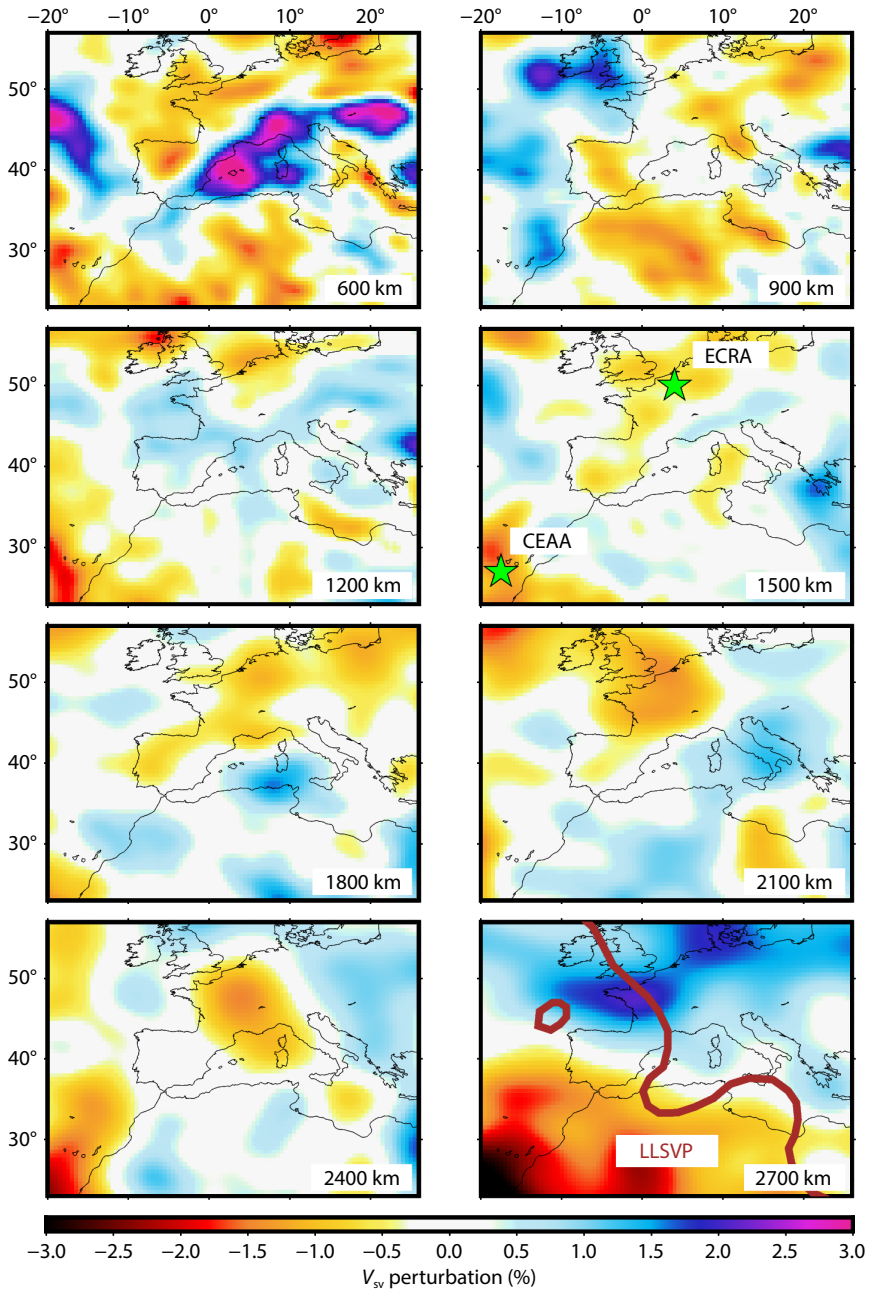

Figure 3. V_{sv} variations from the average wave speed at different depth slices, as imaged by the REVEAL model (Thrastarson et al., 2024). The two green stars in the 1500 km depth slice mark the approximate centers of the CEAA and ECRA low-velocity anomalies. In the 2700 km depth slice, the thick brown line outlines the margins of the African Large Low Shear Velocity Province (LLSVP) as inferred from the tomography model of Simmons et al. (2012).

the Canary Islands, already identified as the Central-East Atlantic Anomaly (CEAA) in Civiero et al. (2021, 2023), which extends down to the core-mantle boundary. At shallower lower-mantle depths (~1200–1800 km), the CEAA persists beneath the western Canary Islands and another large semi-circular low-velocity anomaly with a diameter of ~1000 km appears below the ECRIS in Central Europe. The extension of this second body—that we name European Cenozoic Rift Anomaly (ECRA)—is shown in Figure 4 through two cross-sections oriented in different directions. ECRA appears to be connected to the CEAA in the lowermost mantle and slightly tilted towards the northeast. Another interesting feature in the model is a continuous, elongated low-velocity structure observed in the upper mantle at ~150 km depth extending from the Canary Islands to Western Europe and the Mediterranean Sea.

To complement our tomographic analysis, we identify consistent mantle structures in "vote maps", which facilitate a direct and clear comparison of multiple models at various depths, providing a comprehensive view of the mantle's large-scale features across different datasets (Shephard et al., 2017, 2021). Using this approach, regions with seismic velocity anomalies lower (or higher) than the mean of the negative (or positive) values are

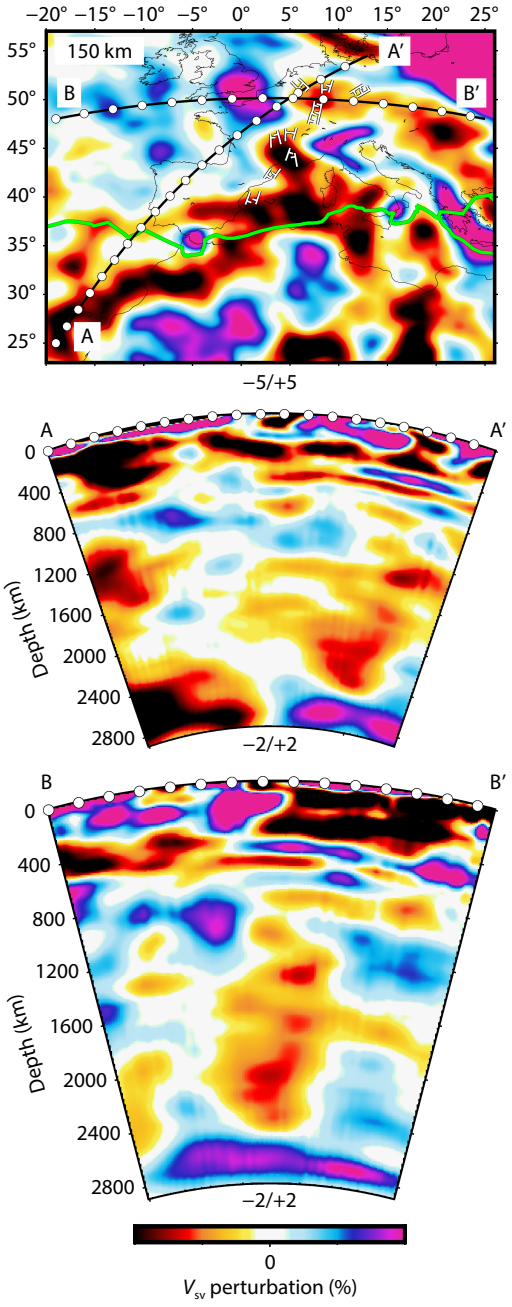

Figure 4. Two cross-sections of the REVEAL model (Thrastarson et al., 2024) showing the CEAA and ECRA low-velocity anomalies from different orientations. Cross-section A–A′ illustrates that the CEAA extends vertically from the core-mantle boundary (CMB) upward, while the ECRA appears connected to it but slightly tilted. Cross-section B–B′, cutting across North-Central Europe, highlights the continuity of the low-velocity anomaly up to mantle transition zone depths. The map view at 150 km depth shows relative V_{sv} variations from the average wave speed at that depth level. Plate boundaries are displayed as green lines, and rifting features (as in Figure 1) are indicated in white.

assigned a value of one, while the remaining regions are assigned a value of zero. Maps for selected tomographic models are then summed at a given depth (Shephard et al., 2017). The resulting vote maps represent the number of selected models that agree on robust structures and do not introduce new features absent in the original tomographic models. Higher vote counts highlight features common across multiple models, whereas lower counts show features present in fewer models. It is important to note that low vote counts do not imply that the features do not exist.

Vote analyses have limitations, as the tomographic models used for vote analysis differ significantly in their construction and resolving power. These differences include: (i) reliance on either S or P waves; (ii) the use of different 1-D reference models, seismic sources, seismograms, and phase-picking techniques; and (iii) variations in inversion domain decompositions, methodologies, and parameterizations (Cottaar and Lekic, 2016; Shephard et al., 2017; Marignier et al., 2020). Moreover, vote images are only as robust as the tomographic models they are based on. The varying degrees of data overlap and parameterization introduce biases, as the votes are not fully independent. Despite these limitations in combining the information from multiple tomography models, vote images remain a useful tool for identifying common large-scale features—such as size, geometry, and position—in tomography.

The vote maps are generated from the SubMachine website (https://users.earth.ox.ac.uk/~smachine, Hosseini et al., 2018), focusing on a set of six whole-mantle S-wave tomographic models (Figure 5). We select deviations from the mean for low-velocity anomalies for the following models: GyPuM-S (Simmons et al., 2010), S362ANI+M (Moulik and Ekström, 2014), S40RTS (Ritsema et al., 2011), Savani (Auer et al., 2014), SEMUCB-WM1 (French and Romanowicz, 2014), and SPani-S (Tesoniero et al., 2015). In this analysis, the vote maps indicate agreement across models about the presence of slow seismic large-scale anomalies (which are interpreted as large-scale plumes) in a depth range that captures the mantle transition zone (MTZ) and the lower mantle.

To highlight robust high-velocity structures, commonly interpreted as subducted lithosphere, we also include in the Supplementary Figure S1 high-velocity vote maps compiled from the following six global P-wave models: DETOX-P3 (Hosseini et al., 2020), GyPSuM-P (Simmons et al., 2010), LLNL_G3Dv3 (Simmons et al., 2012), SPani-P (Tesoniero et al., 2015), UU-P07 (Amaru, 2007), and TX2019slab-P (Lu C et al., 2019). The key characteristics of each model (i.e. data type, seismic phases employed, and native model parametrization) are summarized in Supplementary Table T1.

The vote analysis reinforces the robustness and consistency of the observations across various tomographic datasets. The overall pattern of the seismically slow regions shown in Figure 5 highlights the agreement across tomographic models on the extent of both CEAA and ECRA, as imaged independently by REVEAL. Cross-sections AA′ and BB′ indicate that ECRA connects with CEAA through a thick (~800 km) low-velocity layer near the bottom of the lower mantle. Also, according to Figure S1, we observe a wide high-velocity anomaly within the MTZ encompassing most of the Euro-Mediterranean region, and in particular the area interested by the Alpine orogeny. It has been suggested that this high-velocity material could be the remnant of the Tethyan oceanic lithosphere stagnating in the MTZ below Europe (Marquering and Snieder,

1996; Piromallo and Morelli, 2003).

In Figure S2, we present the map views at the same depths as those in Figure 5 but using a less strict zero threshold metric (dv/v < 0). As expected, also for this threshold, the standout regions where the models highly agree on the presence of slow seismic anomalies are larger than those identified using the 'mean' metric. We also compute the resulting average model at the same depths obtained through *SubMachine* normalizing the average amplitudes of the six S-wave models GyPuM-S, S362ANI+M, S40RTS, Savani, SEMUCB-WM1, and SPani-S (Figure S3). In these images, CEAA and

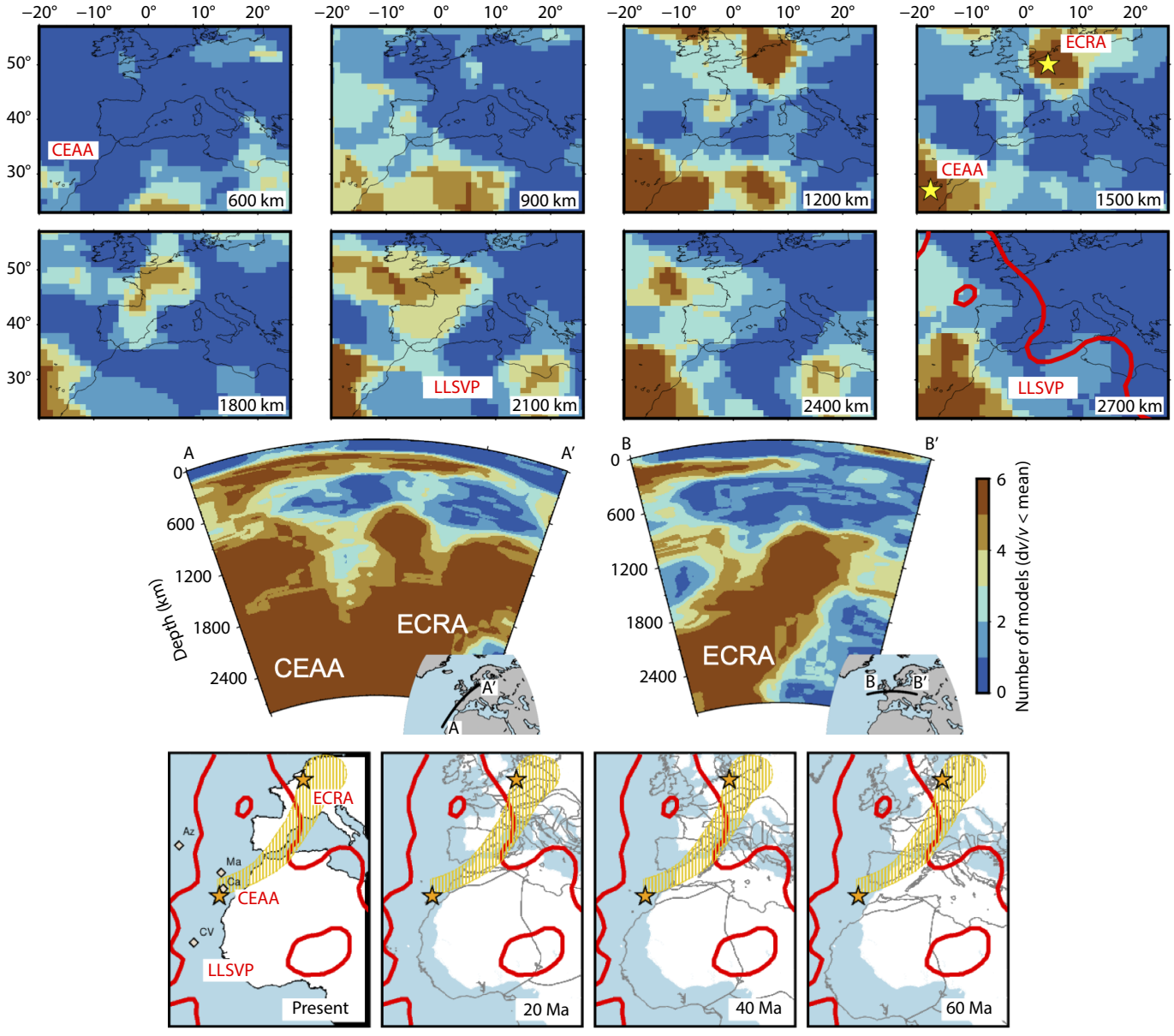

Figure 5. *Top four rows:* Low-velocity vote maps of the whole mantle based on six S-wave tomographic models (dv/v < mean). These maps are obtained by the joint analysis of S-wave models available in the *SubMachine* tomography repository (https://users.earth.ox.ac.uk/~smachine). The vote maps confirm the presence of a broad low-velocity anomaly centered below the Canary Islands (CEAA) through the lower mantle, which may indicate the deep mantle source of the hotspot volcanism. Another low-velocity feature below Central-East Europe (ECRA) underlies the ECRIS and associated volcanism and is likely to be its deep root. *Fifth row:* Vote cross-sections through the Canary Islands and Western-Central Europe. The orientations of the cross-sections are plotted in the inset panels on the bottom right. Note that both CEAA and ECRA appear as broad, deep-seated low-velocity anomalies extending through the lower mantle and merging near the core-mantle boundary. *Bottom row:* GPlates-based plate reconstruction of the Central-East Atlantic Ocean, NW Africa, and Europe from 60 Ma to the present using the EarthByte Rotation File (Zahirovic et al., 2022) released with Gplates version 2.5.0. The stars mark the present-day locations of the CEAA and ECRA. The Macaronesia hotspots (CV: Cape Verde; Ca: Canary Islands; Ma: Madeira; AZ: Azores) are indicated in the first panel with grey diamonds. The boundary of the African LLSVP, inferred from the GyPSuM tomography model (Simmons et al., 2012), is denoted by the thick red line. The yellow shading highlights the spatial distribution of the Cenozoic magmatism. The gray areas correspond to the reconstructed positions of tectonic plates at each time step.

ECRA are two distinct features at mid-mantle depths and merge at ~2400 km depth confirming the existence of two broad anomalies extending up from a unique root. The vertical profiles of the seismic perturbation right below CEAA and ECRA (Figure S4) indicate that the low-velocity layer is continuous in the lowermost mantle beneath the Canary Islands and Western Europe, but disappears below Central Europe. This trend suggests that the common root zone is located offshore in the Central-East Atlantic.

The hot layer falls within the borders of the African Large Low-Shear-Velocity Province (LLSVP) in the lowermost mantle. The LLSVP stretches in the north–south direction from the Northern Atlantic Ocean to the Southwest Indian Ocean (Ni SD and Helmberger, 2003) and has been proposed to have been relatively stable during the last 300 Ma due to its thermo-chemical nature (Torsvik et al., 2014). Assuming the LLSVP has remained stationary, we use GPlates (Müller et al., 2018) to reconstruct the past locations of Cenozoic volcanism relative to it, from the Cenozoic to the present (Figure 5, bottom row). Note that rather than displaying individual volcanic fields, we represent the reconstructed paleo-position of Cenozoic volcanism as an area encompassing all volcanic fields. This region, bounded by the two instabilities (CEAA and ECRA), consistently extends into or near the margins of the LLSVP in the lower mantle from at least 60 Ma to the present.

3. Discussion

The formation of the ECRIS remains a subject of great debate (e.g., Sengör, 1976; Ziegler, 1982; Michon et al., 2003; Dèzes et al., 2004; Bourgeois et al., 2007; Luijendijk et al., 2011; Mouthereau et al., 2021). Distinct models have been proposed to find a single plate-scale mechanism that can explain the Cenozoic rift-related volcanism ranging from active rifting driven by one large or multiple plumes (Granet et al., 1995; Oyarzun et al., 1997; Goes et al., 1999; Ritter et al., 2001) to passive rifting possibly induced by foreland splitting due to the Alpine compression (Sengör, 1976; Dewey and Windley, 1988; Dèzes et al., 2004; Ziegler and Dèzes, 2005), back-arc extension (Jowett, 1991) or slab-pull forces (Stampfli et al., 1998; Michon and Merle, 2001; Michon et al., 2003).

Seismic tomography images asthenospheric P- and S-wave low-velocity anomalies under Western-Central Europe (Granet et al., 1995; Bijwaard et al., 1998; Goes et al., 1999; Ritter et al., 2001; Koulakov et al., 2009), which require the presence of partial melt to be compatible with the observed high surface heat flow (Figure 2). Development of these anomalies during the Paleocene, interpreted as "baby plumes", was associated with an increase in the potential temperature of the asthenosphere (Goes et al., 2000a, b) that, in turn, caused thermal weakening of the foreland lithosphere and localization of the magmatic activity in the ECRIS area.

Here, we provide seismic evidence of the existence of a large low-velocity anomaly, referred to as ECRA, in the mid-mantle below the European continent (Figures 3–5). The consistency of the tomography images, combined with paleo-reconstruction interpretations, suggests that ECRA is a broad-scale, long-lived plume that supplies heat and possibly hot material for the upper-mantle upwellings. The ages of ECRIS volcanism indicate that the plume predates the complete development of subduction in the Mediterranean (Figure 1). Consequently, in the upper mantle, the ECRA material may have been gradually displaced by the subduction of the cold slab allowing weaker "baby plumes" to impinge at the base of the lithosphere in the surrounding areas and trigger localized volcanic activity. Regional uplift above the massifs (Dèzes et al., 2004; Van Camp et al., 2011; Kreemer et al., 2020) may be the result of stresses induced by the relatively hot and buoyant mantle at the bottom of the lithosphere under the volcanic fields. Additionally, local extension due to passive forces could have facilitated the ascent of plume material and the generation of small-scale volcanism in other regions. In this scenario, the age of the alkaline volcanism is determined by the tectonic regime, rather than the plume itself.

In the lowermost mantle, ECRA is connected to the dome-like structure beneath the Canary Islands (CEAA) via a hot, ~800-km-high layer that is part of the LLSVP, with CEAA extending upward into the upper mantle. Regional tomography models show that this instability, interpreted as another broad plume, stalls beneath the MTZ and generates diapiric upper-mantle plumelets beneath the Canary and Madeira hotspot provinces (Civiero et al., 2018, 2019). The plume origin is also supported by a recent shear-wave splitting analysis (Schlaphorst et al., 2022), which shows a radial and heterogeneous anisotropy different from the regional pattern. Receiver functions find a thin MTZ (~220–230 km), the presence of an X discontinuity, and a high basalt fraction (Bonatto et al., 2024) providing additional compelling evidence for a deep-seated thermochemical plume that crosses the MTZ beneath the Canaries.

It has also been suggested that the hot material fueling the volcanism along the Hot Moroccan Line and ECRIS originates from a plume centered beneath the Canary Islands and channeled at sub-lithospheric depths toward western North Africa and Europe (Hoernle et al., 1995; Piromallo et al., 2008; Duggen et al., 2009; Mériaux et al., 2015). Oyarzun et al. (1997) propose that the first plume-suction event occurred during the Late Cretaceous opening of the southern branch of the North Atlantic while the second event—the formation of the ECRIS—allowed the final north-northeast-directed pervasion of the European domain by the long-lived plume material and alkaline volcanism. In the REVEAL model (Figure 4), we observe an elongated low-velocity feature that extends from the Canary archipelago to Morocco and the Mediterranean terminating around the Massif Central. While this supports the possibility of relatively geochemically uniform material spreading across the shallow sub-lithospheric mantle beneath North Africa and Western Europe, which could explain the alkaline activity in these regions, the hypothesis does not account for the Central European volcanism (e.g., Bohemian Massif, Rhenish Massif, Heagu-Urach volcanic area, see Figure 1). To address this, we propose that the alternative source is the ECRA plume, which we identify in this study.

In conclusion, we attribute the low-velocity layer at the bottom of the mantle to the northern part of the African LLSVP, as indicated by many global tomography models (e.g., Simmons et al., 2012; Auer et al., 2014; French and Romanowicz, 2014). This region serves as a common root for the CEAA and ECRA plumes, which ascend to the base of the MTZ, possibly triggering much narrower upper-mantle upwellings. The localized nature of scattered, small-

scale volcanism across the province (Figure 1c) reflects tectonic control on magmatic upwelling paths. In this context, we provide evidence for a lower-mantle source feeding these upper-mantle upwellings, which was not recognized in Lustrino and Wilson (2007)'s model. The little variations of the geochemical characteristics of the volcanic fields across the region can be seen as a function of lithospheric heterogeneities within different terrane blocks (Wilson and Downes, 1991).

The interaction of the upper-mantle plume material with subducted material under southern Europe and the predominantly compressive European stress regime (Carafa and Barba, 2013) may have prevented the progress of the rift development and the formation of a great amount of volcanism, as observed in other rifting zones like the Afro-Arabian rift system or in Iceland.

The role of the Alpine subducted slab in regulating mantle flow and its potential impact on volcanic activity in Europe remains an important area for future research. 4-D numerical modeling applied to a similar tectonic setting, such as the Yellowstone volcanic province in western U.S.—where a mantle plume interacts with the Farallon subduction—shows that the slab consistently obstructs its ascent. The plume could only reach the surface after interacting with the broken slab hinge around 15 Ma, as shown by Leonard and Liu LJ (2016). Consequently, the conventional plume model fails to predict the presence of voluminous hot materials at shallow depths beneath the region, indicating that the dynamics of plume rise is more complex than previously thought.

In the context of European Cenozoic volcanism, testing whether a similar mechanism might be at play is essential. Geodynamic models, particularly those that incorporate data assimilation techniques as demonstrated by Zhou Q et al. (2018), will be critical in assessing the extent to which mantle plumes contribute to the alkaline volcanism observed in the ECRIS. These models can help refine our understanding of mantle dynamics and their interaction with subducted slabs, providing a more comprehensive view of the forces shaping Earth's volcanic regions.

4. Final Remarks

Seismic tomography results support the hypothesis that a broad plume (ECRA) originates from a lowermost mantle source beneath the Eastern Atlantic, providing a plausible geodynamic framework for the alkaline volcanic activity in Western-Central Europe. While plate-boundary forces are crucial in driving Cenozoic rifting in Europe, regional mantle structure also plays a significant role in modulating stress variations, intraplate tectonic styles, and volcanic activity. Future high-resolution, whole-mantle tomography studies, combined with geodynamic modeling, should further elucidate the relationship between the ECRA plume, asthenospheric upwellings across Europe, and the subducted Alpine lithosphere.

Declaration of Competing Interest

The authors declare that she has no known competing financial interests or personal relationships that could have appeared to influence the work reported in this paper.

Acknowledgments

The authors thank Andrea Marzoli for discussions on the geochemistry of the volcanic rocks and Magdala Tesauro for proofreading. All figures were created using Generic Mapping Tools (GMT; Wessel et al., 2019). This work is supported by grant D86-RALMI23CIVIE_01 awarded by the Italian Ministry of University and Research under the Program for Young Researchers "Rita Levi Montalcini".

References

Amaru, M. L. (2007). Global travel time tomography with 3-D reference models. *Geol. Ultraiectina*, *274*, 174.

Auer, L., Boschi, L., Becker, T. W., Nissen-Meyer, T., and Giardini, D. (2014). *Savani*: A variable resolution whole-mantle model of anisotropic shear velocity variations based on multiple data sets. *J. Geophys. Res.: Solid Earth*, *119*(4), 3006–3034. https://doi.org/10.1002/2013JB010773

Bijwaard, H., Spakman, W., and Engdahl, E. R. (1998). Closing the gap between regional and global travel time tomography. *J. Geophys. Res.: Solid Earth*, *103*(B12), 30055–30078. https://doi.org/10.1029/98JB02467

Bonatto, L., Schlaphorst, D., Silveira, G., Mata, J., Civiero, C., Piromallo, C., and Schimmel, M. (2024). Unveiling the distinct structure of the upper mantle beneath the Canary and Madeira Hotspots, as depicted by the 660, 410, and X discontinuities. *J. Geophys. Res.: Solid Earth*, *129*(5), e2023JB028195. https://doi.org/10.1029/2023JB028195

Boschi, L., Becker, T. W., and Steinberger, B. (2007). Mantle plumes: Dynamic models and seismic images. *Geochem. Geophys. Geosyst.*, *8*(10), Q10006. https://doi.org/10.1029/2007GC001733

Bourgeois, O., Ford, M., Diraison, M., Le Carlier de Veslud, C., Gerbault, M., Pik, R., Ruby, N., and Bonnet, S. (2007). Separation of rifting and lithospheric folding signatures in the NW-Alpine foreland. *Int. J. Earth Sci.*, *96*(6), 1003–1031. https://doi.org/10.1007/s00531-007-0202-2

Buikin, A., Trieloff, M., Hopp, J., Althaus, T., Korochantseva, E., Schwarz, W. H., and Altherr, R. (2005). Noble gas isotopes suggest deep mantle plume source of late Cenozoic mafic alkaline volcanism in Europe. *Earth Planet. Sci. Lett.*, *230*(1-2), 143–162. https://doi.org/10.1016/j.epsl.2004.11.001

Carafa, M. M. C., and Barba, S. (2013). The stress field in Europe: optimal orientations with confidence limits. *Geophys. J. Int.*, *193*(2), 531–548. https://doi.org/10.1093/gji/ggt024

Civiero, C., Strak, V., Custódio, S., Silveira, G., Rawlinson, N., Arroucau, P., and Corela, C. (2018). A common deep source for upper-mantle upwellings below the Ibero-western Maghreb region from teleseismic *P*-wave travel-time tomography. *Earth Planet. Sci. Lett.*, *499*, 157–172. https://doi.org/10.1016/J.EPSL.2018.07.024

Civiero, C., Custódio, S., Rawlinson, N., Strak, V., Silveira, G., Arroucau, P., and Corela, C. (2019). Thermal nature of mantle upwellings below the Ibero-western Maghreb region inferred from teleseismic tomography. *J. Geophys. Res.: Solid Earth*, *124*(2), 1781–1801. https://doi.org/10.1029/2018JB016531

Civiero, C., Custódio, S., Neres, M., Schlaphorst, D., Mata, J., and Silveira, G. (2021). The role of the seismically slow Central-East Atlantic Anomaly in the genesis of the Canary and Madeira volcanic provinces. *Geophys. Res. Lett.*, *48*(13), e2021GL092874. https://doi.org/10.1029/2021gl092874

Civiero, C., Carvalho, J., and Silveira, G. (2023). Mantle structure beneath the Macaronesian volcanic islands (Cape Verde, Canaries, Madeira and Azores): A review and future directions. *Front. Earth Sci.*, *11*, 1126274. https://doi.org/10.3389/feart.2023.1126274

Comas, M. C., García-Dueñas, V., and Jurado, M. J. (1992). Neogene tectonic evolution of the Alboran Sea from MCS data. *Geo-Mar. Lett.*, *12*(2-3), 157–164. https://doi.org/10.1007/BF02084927

Cottaar, S., and Lekic, V. (2016). Morphology of seismically slow lower-mantle structures. *Geophys. J. Int.*, *207*(2), 1122–1136. https://doi.org/10.1093/gji/ggw324

Dewey, J. F., and Windley, B. F. (1988). Palaeocene-Oligocene tectonics of NW Europe. *Geol. Soc. London Spec. Publ.*, *39*(1), 25–31. https://doi.org/10.1144/GSL.SP.1988.039.01.04

Dèzes, P., Schmid, S. M., and Ziegler, P. A. (2004). Evolution of the European Cenozoic Rift System: interaction of the Alpine and Pyrenean orogens with their foreland lithosphere. *Tectonophysics*, *389*(1-2), 1–33. https://doi.org/10.1016/j.tecto.2004.06.011

Duggen, S., Hoernle, K. A., Hauff, F., Klügel, A., Bouabdellah, M., and Thirlwall, M. F. (2009). Flow of Canary mantle plume material through a subcontinental lithospheric corridor beneath Africa to the Mediterranean. *Geology*, *37*(3), 283–286. https://doi.org/10.1130/G25426A.1

Fichtner, A., and Villaseñor, A. (2015). Crust and upper mantle of the western Mediterranean – Constraints from full-waveform inversion. *Earth Planet. Sci. Lett.*, *428*, 52–62. https://doi.org/10.1016/j.epsl.2015.07.038

French, S. W., and Romanowicz, B. A. (2014). Whole-mantle radially anisotropic shear velocity structure from spectral-element waveform tomography. *Geophys. J. Int.*, *199*(3), 1303–1327. https://doi.org/10.1093/gji/ggu334

Frizon de Lamotte, D., Leturmy, P., Missenard, Y., Khomsi, S., Ruiz, G., Saddiqi, O., Guillocheau, F., and Michard, A. (2009). Mesozoic and Cenozoic vertical movements in the Atlas system (Algeria, Morocco, Tunisia): An overview. *Tectonophysics*, *475*(1), 9–28. https://doi.org/10.1016/j.tecto.2008.10.024

Fuchs, S., Norden, B., and International Heat Flow Commission. (2021). The Global Heat Flow Database: Release 2021. GFZ Data Services. https://doi.org/10.5880/fidgeo.2021.014

Fullea, J., Lebedev, S., Martinec, Z., and Celli, N. L. (2021). WINTERC-G: mapping the upper mantle thermochemical heterogeneity from coupled geophysical-petrological inversion of seismic waveforms, heat flow, surface elevation and gravity satellite data. *Geophys. J. Int.*, *226*(1), 146–191. https://doi.org/10.1093/gji/ggab094

Goes, S., Spakman, W., and Bijwaard, H. (1999). A lower mantle source for central European volcanism. *Science*, *286*(5446), 1928–1931. https://doi.org/10.1126/science.286.5446.1928

Goes, S., Govers, R., and Vacher, P. (2000a). Shallow mantle temperatures under Europe from *P* and *S* wave tomography. *J. Geophys. Res.: Solid Earth*, *105*(B5), 11153–11169. https://doi.org/10.1029/1999jb900300

Goes, S., Loohuis, J. J. P., Wortel, M. J. R., and Govers, R. (2000b). The effect of plate stresses and shallow mantle temperatures on tectonics of northwestern Europe. *Glob. Planet. Change*, *27*(1-4), 23–38. https://doi.org/10.1016/S0921-8181(01)00057-1

Granet, M., Wilson, M., and Achauer, U. (1995). Imaging a mantle plume beneath the French Massif Central. *Earth Planet. Sci. Lett.*, *136*(3-4), 281–296. https://doi.org/10.1016/0012-821X(95)00174-B

Haase, K. M., Goldschmidt, B., and Garbe-Schönberg, C. D. (2004). Petrogenesis of tertiary continental intra-plate lavas from the Westerwald region, Germany. *J. Petrol.*, *45*(5), 883–905. https://doi.org/10.1093/petrology/egg115

Harangi, S., Downes, H., and Seghedi, I. (2006). Tertiary-Quaternary subduction processes and related magmatism in the Alpine-Mediterranean region. *Memoirs*, *32*(1), 167–190. https://doi.org/10.1144/GSL.MEM.2006.032.01.10

Hoernle, K., Zhang, Y. S., and Graham, D. (1995). Seismic and geochemical evidence for large-scale mantle upwelling beneath the eastern Atlantic and western and central Europe. *Nature*, *374*(6517), 34–39. https://doi.org/10.1038/374034a0

Hosseini, K., Matthews, K. J., Sigloch, K., Shephard, G. E., Domeier, M., and Tsekhmistrenko, M. (2018). SubMachine: Web-based tools for exploring seismic tomography and other models of Earth's deep interior. *Geochem. Geophys. Geosyst.*, *19*(5), 1464–1483. https://doi.org/10.1029/2018GC007431

Hosseini, K., Sigloch, K., Tsekhmistrenko, M., Zaheri, A., Nissen-Meyer, T., and Igel, H. (2020). Global mantle structure from multifrequency tomography using *P*, *PP* and *P*-diffracted waves. *Geophys. J. Int.*, *220*(1), 96–141. https://doi.org/10.1093/gji/ggz394

Huismans, R. S., Podladchikov, Y. Y., and Cloetingh, S. (2001). Transition from passive to active rifting: Relative importance of asthenospheric doming and passive extension of the lithosphere. *J. Geophys. Res.: Solid Earth*, *106*(B6), 11271–11291. https://doi.org/10.1029/2000JB900424

Jolivet, L., Faccenna, C., D'Agostino, N., Fournier, M., and Worrall, D. (1999). The kinematics of back-arc basins, examples from the Tyrrhenian, Aegean and Japan Seas. *Geol. Soc. London Spec. Publ.*, *164*(1), 21–53. https://doi.org/10.1144/GSL.SP.1999.164.01.04

Jowett, E. C. (1991). Post-collisional formation of the Alpine foreland rifts. *Ann. Soc. Geol. Polon.*, *61*(1-2), 37–59.

Koptev, A., Cloetingh, S., and Ehlers, T. A. (2021). Longevity of small-scale ('baby') plumes and their role in lithospheric break-up. *Geophys. J. Int.*, *227*(1), 439–471. https://doi.org/10.1093/gji/ggab223

Koulakov, I., Kaban, M. K., Tesauro, M., and Cloetingh, S. (2009). *P*- and *S*-velocity anomalies in the upper mantle beneath Europe from tomographic inversion of ISC data. *Geophys. J. Int.*, *179*(1), 345–366. https://doi.org/10.1111/j.1365-246X.2009.04279.x

Kreemer, C., Blewitt, G., and Davis, P. M. (2020). Geodetic evidence for a buoyant mantle plume beneath the Eifel volcanic area, NW Europe. *Geophys. J. Int.*, *222*(2), 1316–1332. https://doi.org/10.1093/gji/ggaa227

Leonard, T., and Liu, L. J. (2016). The role of a mantle plume in the formation of Yellowstone volcanism. *Geophys. Res. Lett.*, *43*(3), 1132–1139. https://doi.org/10.1002/2015GL067131

Liu, Q., and Gu, Y. J. (2012). Seismic imaging: From classical to adjoint tomography. *Tectonophysics, 566–567*, 31–66. https://doi.org/10.1016/j.tecto.2012.07.006

Lonergan, L., and White, N. (1997). Origin of the Betic-Rif mountain belt. *Tectonics*, *16*(3), 504–522. https://doi.org/10.1029/96TC03937

Lu, C., Grand, S. P., Lai, H. Y., and Garnero, E. J. (2019). TX2019slab: A new *P* and *S* tomography model incorporating subducting slabs. *J. Geophys. Res.: Solid Earth*, *124*(11), 11549–11567. https://doi.org/10.1029/2019JB017448

Luijendijk, E., ter Voorde, M., van Balen, R., Verweij, H., and Simmelink, E. (2011). Thermal state of the Roer Valley Graben, part of the European Cenozoic Rift System. *Basin Res.*, *23*(1), 65–82. https://doi.org/10.1111/j.1365-2117.2010.00466.x

Lustrino, M., and Wilson, M. (2007). The circum-Mediterranean anorogenic Cenozoic igneous province. *Earth-Sci. Rev.*, *81*(1-2), 1–65. https://doi.org/10.1016/j.earscirev.2006.09.002

Marignier, A., Ferreira, A. M. G., and Kitching, T. (2020). The probability of mantle plumes in global tomographic models. *Geochem. Geophys. Geosyst.*, *21*(9), e2020GC009276. https://doi.org/10.1029/2020GC009276

Marquering, H., and Snieder, R. (1996). Shear-wave velocity structure beneath Europe, the northeastern Atlantic and western Asia from waveform inversions including surface-wave mode coupling. *Geophys. J. Int.*, *127*(2), 283–304. https://doi.org/10.1111/j.1365-246X.1996.tb04720.x

Masters, G., Jordan, T. H., Silver, P. G., and Gilbert, F. (1982). Aspherical Earth structure from fundamental spheroidal-mode data. *Nature*, *298*(5875), 609–613. https://doi.org/10.1038/298609a0

McKenzie, D., and Bickle, M. J. (1988). The volume and composition of melt generated by extension of the lithosphere. *J. Petrol.*, *29*(3), 625–679. https://doi.org/10.1093/petrology/29.3.625

Mériaux, C. A., Duarte, J. C., Duarte, S. S., Schellart, W. P., Chen, Z., Rosas, F., Mata, J., and Terrinha, P. (2015). Capture of the Canary mantle plume material by the Gibraltar arc mantle wedge during slab rollback. *Geophys. J. Int.*, *201*(3), 1717–1721. https://doi.org/10.1093/gji/ggv120

Merle, O. (2011). A simple continental rift classification. *Tectonophysics*, *513*(1-4), 88–95. https://doi.org/10.1016/j.tecto.2011.10.004

Michon, L., and Merle, O. (2001). The evolution of the Massif Central Rift; spatio-temporal distribution of the volcanism. *Bull. Soc. Géol. France*, *172*(2), 201–211. https://doi.org/10.2113/172.2.201

Michon, L., Van Balen, R. T., Merle, O., and Pagnier, H. (2003). The Cenozoic evolution of the Roer Valley Rift System integrated at a European scale. *Tectonophysics*, *367*(1-2), 101–126. https://doi.org/10.1016/S0040-1951(03)00132-X

Moulik, P., and Ekström, G. (2014). An anisotropic shear velocity model of the Earth's mantle using normal modes, body waves, surface waves and long-period waveforms. *Geophys. J. Int.*, *199*(3), 1713–1738. https://doi.org/10.1093/gji/ggu356

Mouthereau, F., Angrand, P., Jourdon, A., Ternois, S., Fillon, C., Calassou, S., Chevrot, S., Ford, M., Jolivet, L., … Baudin, T. (2021). Cenozoic mountain building and topographic evolution in Western Europe: impact of billions of years of lithosphere evolution and plate kinematics. *Bull. Soc. Géol. France*, *192*(1), 56. https://doi.org/10.1051/bsgf/2021040

Müller, R. D., Cannon, J., Qin, X. D., Watson, R. J., Gurnis, M., Williams, S., Pfaffelmoser, T., Seton, M., Russell, S. H. J., and Zahirovic, S. (2018). GPlates: Building a virtual earth through deep time. *Geochem. Geophys. Geosyst.*, *19*(7), 2243–2261. https://doi.org/10.1029/2018GC007584

Ni, S. D., and Helmberger, D. V. (2003). Ridge-like lower mantle structure beneath South Africa. *J. Geophys. Res.: Solid Earth*, *108*(B2), 2094. https://doi.org/10.1029/2001JB001545

Oyarzun, R., Doblas, M., López-Ruiz, J., and Cebrá, J. M. (1997). Opening of the central Atlantic and asymmetric mantle upwelling phenomena: Implications for long-lived magmatism in western North Africa and Europe. *Geology*, *25*(8), 727–730. https://doi.org/10.1130/0091-7613(1997)025<0727:OOTCAA>2.3.CO;2

Piromallo, C., and Morelli, A. (2003). *P* wave tomography of the mantle under the Alpine-Mediterranean area. *J. Geophys. Res.: Solid Earth*, *108*(B2), 2065. https://doi.org/10.1029/2002JB001757

Piromallo, C., Gasperini, D., Macera, P., and Faccenna, C. (2008). A late Cretaceous contamination episode of the European–Mediterranean mantle. *Earth Planet. Sci. Lett.*, *268*(1-2), 15–27. https://doi.org/10.1016/j.epsl.2007.12.019

Plomerová, J., Achauer, U., Babuška, V., Vecsey, L., and BOHEMA Working Group. (2007). Upper mantle beneath the Eger Rift (Central Europe): Plume or asthenosphere upwelling?. *Geophys. J. Int.*, *169*(2), 675–682. https://doi.org/10.1111/j.1365-246X.2007.03361.x

Rawlinson, N., and Sambridge, M. (2004). Wave front evolution in strongly heterogeneous layered media using the fast marching method. *Geophys. J. Int.*, *156*(3), 631–647. https://doi.org/10.1111/j.1365-246X.2004.02153.x

Ritsema, J., Deuss, A., van Heijst, H. J., and Woodhouse, J. H. (2011). S40RTS: a degree-40 shear-velocity model for the mantle from new Rayleigh wave dispersion, teleseismic traveltime and normal-mode splitting function measurements. *Geophys. J. Int.*, *184*(3), 1223–1236. https://doi.org/10.1111/j.1365-246X.2010.04884.x

Ritter, J. R. R., Jordan, M., Christensen, U. R., and Achauer, U. (2001). A mantle plume below the Eifel volcanic fields, Germany. *Earth Planet. Sci. Lett.*, *186*(1), 7–14. https://doi.org/10.1016/S0012-821X(01)00226-6

Ruppel, C. (1995). Extensional processes in continental lithosphere. *J. Geophys. Res.: Solid Earth*, *100*(B12), 24187–24215. https://doi.org/10.1029/95JB02955

Schlaphorst, D., Silveira, G., Mata, J., Krüger, F., Dahm, T., and Ferreira, A. M. G. (2022). Heterogeneous seismic anisotropy beneath Madeira and Canary archipelagos revealed by local and teleseismic shear wave splitting. *Geophys. J. Int.*, *233*(1), 510–528. https://doi.org/10.1093/gji/ggac472

Sengör, A. M. C. (1976). Collision of irregular continental margins: Implications for foreland deformation of Alpine-type orogens. *Geology*, *4*(12), 779–782. https://doi.org/10.1130/0091-7613(1976)4<779:COICMI>2.0.CO;2

Sengör, A. M. C., and Burke, K. (1978). Relative timing of rifting and volcanism on Earth and its tectonic implications. *Geophys. Res. Lett.*, *5*(6), 419–421. https://doi.org/10.1029/GL005i006p00419

Shephard, G. E., Matthews, K. J., Hosseini, K., and Domeier, M. (2017). On the consistency of seismically imaged lower mantle slabs. *Sci. Rep.*, *7*(1), 10976. https://doi.org/10.1038/s41598-017-11039-w

Shephard, G. E., Houser, C., Hernlund, J. W., Valencia-Cardona, J. J., Trønnes, R. G., and Wentzcovitch, R. M. (2021). Seismological expression of the iron spin crossover in ferropericlase in the Earth's lower mantle. *Nat. Commun.*, *12*(1), 5905. https://doi.org/10.1038/s41467-021-26115-z

Simmons, N. A., Forte, A. M., Boschi, L., and Grand, S. P. (2010). GyPSuM: A joint tomographic model of mantle density and seismic wave speeds. *J. Geophys. Res.: Solid Earth*, *115*(B12), B12310. https://doi.org/10.1029/2010JB007631

Simmons, N. A., Myers, S. C., Johannesson, G., and Matzel, E. (2012). LLNL-G3Dv3: Global P wave tomography model for improved regional and teleseismic travel time prediction. *J. Geophys. Res.: Solid Earth*, *117*(B10), B10302. https://doi.org/10.1029/2012JB009525

Spakman, W., van der Lee, S., and van der Hilst, R. (1993). Travel-time tomography of the European-Mediterranean mantle down to 1400 km. *Phys. Earth Planet. Inter.*, *79*(1-2), 3–74. https://doi.org/10.1016/0031-9201(93)90142-V

Stampfli, G. M., Mosar, J., Marquer, D., Marchant, R., Baudin, T., and Borel, G. (1998). Subduction and obduction processes in the Swiss Alps. *Tectonophysics*, *296*(1-2), 159–204. https://doi.org/10.1016/S0040-1951(98)00142-5

Tesoniero, A., Auer, L., Boschi, L., and Cammarano, F. (2015). Hydration of marginal basins and compositional variations within the continental lithospheric mantle inferred from a new global model of shear and compressional velocity. *J. Geophys. Res.: Solid Earth*, *120*(11), 7789–7813. https://doi.org/10.1002/2015JB012026

Thrastarson, S., van Herwaarden, D. P., Noe, S., Josef Schiller, C., and Fichtner, A. (2024). REVEAL: A global full-waveform inversion model. *Bull. Seismol. Soc. Am.*, *114*(3), 1392–1406. https://doi.org/10.1785/0120230273

Torsvik, T. H., van der Voo, R., Doubrovine, P. V., Burke, K., Steinberger, B., Ashwal, L. D., Trønnes, R. G., Webb, S. J., and Bull, A. L. (2014). Deep mantle structure as a reference frame for movements in and on the Earth. *Proc. Natl. Acad. Sci. USA*, *111*(24), 8735–8740. https://doi.org/10.1073/pnas.1318135111

Van Camp, M., de Viron, O., Scherneck, H. G., Hinzen, K. G., Williams, S. D. P., Lecocq, T., Quinif, Y., and Camelbeeck, T. (2011). Repeated absolute gravity measurements for monitoring slow intraplate vertical deformation in western Europe. *J. Geophys. Res.: Solid Earth*, *116*(B8), B08402. https://doi.org/10.1029/2010JB008174

van der Hilst, R. D., Widiyantoro, S., and Engdahl, E. R. (1997). Evidence for deep mantle circulation from global tomography. *Nature*, *386*(6625), 578–584. https://doi.org/10.1038/386578a0

Wedepohl, K. H. (2000). The composition and formation of Miocene tholeiites in the Central European Cenozoic plume volcanism (CECV). *Contrib. Mineral. Petrol.*, *140*(2), 180–189. https://doi.org/10.1007/s004100000184

Wessel, P., Luis, J. F., Uieda, L., Scharroo, R., Wobbe, F., Smith, W. H. F., and Tian, D. (2019). The generic mapping tools version 6. *Geochem. Geophys. Geosyst.*, *20*(11), 5556–5564. https://doi.org/10.1029/2019GC008515

Wilson, M., and Downes, H. (1991). Tertiary-Quarternary extension-related alkaline magmatism in Western and Central Europe. *J. Petrol.*, *32*(4), 811–849. https://doi.org/10.1093/petrology/32.4.811

Wilson, M. (1992). Magmatism and continental rifting during the opening of the South Atlantic Ocean: a consequence of Lower Cretaceous super-plume activity?. *Geol. Soc. London Spec. Publ.*, *68*(1), 241–255. https://doi.org/10.1144/GSL.SP.1992.068.01.15

Zahirovic, S., Eleish, A., Doss, S., Pall, J., Cannon, J., Pistone, M., Tetley, M. G., Young, A., and Fox, P. (2022). Subduction and carbonate platform interactions. *Geosci. Data J.*, *9*(2), 371–383. https://doi.org/10.1002/gdj3.146

Zhou, Q., Liu, L. J., and Hu, J. S. (2018). Western US volcanism due to intruding oceanic mantle driven by ancient Farallon slabs. *Nat. Geosci.*, *11*(1), 70–76. https://doi.org/10.1038/s41561-017-0035-y

Zhu, H. J., Bozdağ, E., and Tromp, J. (2015). Seismic structure of the European upper mantle based on adjoint tomography. *Geophys. J. Int.*, *201*(1), 18–52. https://doi.org/10.1093/gji/ggu492

Ziegler, P. A. (1982). Faulting and graben formation in western and central Europe. *Philos. Trans. Roy. Soc. A: Math. Phys. Eng. Sci.*, *305*(1489), 113–143. https://doi.org/10.1098/rsta.1982.0029

Ziegler, P. A. (1992). European Cenozoic rift system. *Tectonophysics*, *208*(1-3), 91–111. https://doi.org/10.1016/0040-1951(92)90338-7

Ziegler, P. A., and Cloetingh, S. (2004). Dynamic processes controlling evolution of rifted basins. *Earth-Sci. Rev.*, *64*(1-2), 1–50. https://doi.org/10.1016/S0012-8252(03)00041-2

Ziegler, P. A., and Dèzes, P. (2005). Evolution of the lithosphere in the area of the Rhine Rift System. *Int. J. Earth Sci.*, *94*(4), 594–614. https://doi.org/10.1007/s00531-005-0474-3